JOURNAL OF GEOPHYSICAL RESEARCH, VOL. 91, NO. C12, PAGES 14,212–14,220, DECEMBER 15, 1986

The Mass and Heat Budget in a Model of the Tropical Atlantic Ocean

S. G. H. PHILANDER AND R. C. PACANOWSKI

Geophysical Fluid Dynamics Laboratory, NOAA, Princeton University, Princeton, New Jersey

In a general circulation model of the tropical Atlantic Ocean, the northwestward flowing Brazilian Coastal Current is fed by the westward South Equatorial Countercurrent and in turn loses water to the eastward Equatorial Undercurrent and the eastward North Equatorial Countercurrent. The transport of the countercurrent decreases in a downstream direction primarily because of downwelling and then equatorward flow, in the thermocline, into the undercurrent. Some of the countercurrent water penetrates into the Gulf of Guinea, where it flows into the southern hemisphere. The transport of the Equatorial Undercurrent decreases because upwelling, which is most intense in the western side of the basin, transfers fluid into the surface layers to sustain divergent Ekman drift which is swept westward by the South Equatorial Undercurrent. The model has a northward heat transport across all latitudes in the tropics. Seasonal variations in this transport are modest to the south of 5°S and to the north of 15°N. Across 8°N, however, the transport varies from 1.5×10^{15} W in January and February to -0.1×10^{15} W in August. This result implies that the zonal bands 5°S to 8°N and 8°N to 15°N act as capacitors that are out of phase. In July, August, and September the heat gained from the southern hemisphere is stored in the 5°S to 8°N band where the thermocline deepens. During this period (when the Brazilian Coastal Current turns offshore near 5°N) the thermocline between 8°N and 15°N rises as heat is lost across 15°N. When the Brazilian Coastal Current flows continuously along the coast into the Gulf of Mexico, from December into May, it transports heat from the band 5°S to 8°N to replenish the heat stored between 8°N and 15°N and to sustain the heat flux across 15°N.

1. INTRODUCTION

Studies of the oceanic circulation in the tropics have thus far focused on isolated aspects of that circulation, the dynamics of the Equatorial Undercurrent and the North Equatorial Countercurrent, for example. Little attention has been paid to the relation between the different currents and to the closure of the circulation, but there have been attempts to estimate the heat transport associated with this circulation. All estimates involve models because oceanographic data for the direct calculation of the oceanic heat transport are unavailable. The heat transport can only be estimated by using the limited available data together with the equations of motion for the ocean. The various methods that have been devised to do this differ in the degree to which they exploit the equations of motion. One method uses only the equation for the conservation of heat. In its steady state form, this equation can be integrated over an entire polar cap from the pole to a fixed latitude to determine the heat transport across that latitude, provided that the heat flux across the ocean surface is known [*Sverdrup*, 1957; *Bryan*, 1962]. A second method uses only the meridional and vertical momentum equations in simplified form and does not exploit the heat equation at all. Meridional geostrophic currents are calculated from zonal hydrographic sections and are converted to absolute currents by inferring the vertically integrated Sverdrup flow from the wind stress data which also determine the surface Ekman drift. The transport of the western boundary current remains a problem, but if it is assumed to balance the Sverdrup transport across the latitude under consideration, then it is only the width of the western boundary current that has to be specified in a some what arbitrary manner [*Bryan*, 1962, 1982; *Bennett*, 1978; *Hastentrath*, 1980, 1982]. The method devised by *Wunsch* [1980, 1984], *Roemmich* [1983], and others use all the equations of motion, for the conservation of mass, momentum, heat, and salt, together with the available thermal and salinity data from hydrographic sections. (The horizontal momentum equations are used only in geostrophic form, except for a surface Ekman layer.) The resultant equations for the velocity components are indeterminate. Inverse methods select a solution on the basis of a number of arbitrary but "reasonable" constraints. *Roemmich* [1983], for example, demands that the vertically integrated geostrophic transport be equal and opposite to the Ekman transport in the surface layers. Additional constraints imposed by *Wunsch* [1984] amount to upper and lower limits for certain quantities, velocity components as inferred from tracers, for example. These constraints can then be translated into upper and lower limits for the heat flux across different meridians.

The methods for estimating the heat flux mentioned thus far make full use neither of the equations of motion nor of the information available in the surface winds (which do far more than drive Ekman drift). To do this, a general circulation model of the ocean is required. Such a model also eliminates a questionable assumption made in the simpler models, namely, that the meridional flow is geostrophic everywhere below the surface layers, even in low latitudes and in intense boundary currents at an angle to meridians (the Brazilian Coastal Current, for example). The general circulation model is a powerful tool, but it has drawbacks. The two principal problems are the following: in the formulation of the equations of motion the parameterization of mixing processes is arbitrary, and in the (numerical) method of solution of the equations the available computer resources do not permit a numerical grid that resolves all the dynamically important oceanic eddies. Both these problems are less severe in the tropics than in higher latitudes. The numerical grid necessary to resolve the eddies in the tropics is no finer than that needed to resolve the narrow tropical currents, such as the Equatorial Undercurrent. Available

This paper is not subject to U.S. copyright. Published in 1986 by the American Geophysical Union.

Paper number 6C0463.

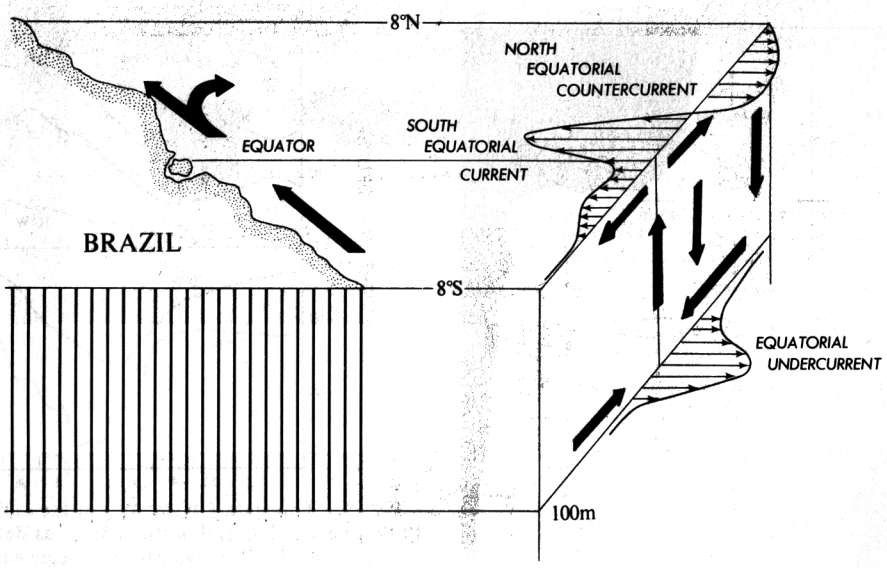

Fig. 1. A schematic diagram of the circulation in the tropical Atlantic Ocean.

computer resources are adequate for such a grid but not for a grid that also resolves eddies in the subtropics and midlatitudes. (The eddies in the tropics are confined to the neighborhood of the equator, are associated with instabilities of the surface currents, and have a horizontal scale of a few hundred kilometers.) Mixing processes are somewhat simpler in the tropics than in high latitudes because deep convective overturning is of secondary importance in low but not in high latitudes. Available parameterizations for mixing by wind stirring and by vertical shear instabilities, in terms of the Richardson number of the flow, are acceptable because models that incorporate these parameterizations are reasonably realistic in the tropics. For example, such models successfully simulate the major changes in the currents and thermal field both in the tropical Pacific Ocean during El Niño of 1982–1983 [*Philander and Seigel*, 1985] and in the tropical Atlantic Ocean during a seasonal cycle [*Philander and Pacanowski*, 1984, this issue]. This success is limited to time scales of up to a few years. On longer time scales, inadequacies of the mixing parameterization result in a downward diffusion of the thermocline. The models are successful at reproducing the response of a given thermocline to wind fluctuations on time scales of up to a few years but are poor at reproducing the processes that maintain the thermocline itself on much longer time scales. In principle only the fluxes of heat and momentum need to be specified as boundary conditions for the models. In practice, data that describe the thermal structure of the ocean are needed as initial conditions.

An improvement over a general circulation model that uses oceanographic measurements merely as initial conditions is a general circulation model that assimilates available data so that the data become constraints on the model. Such a model is yet to be developed.

This paper describes seasonal variations in the mass and heat budgets of the tropical Atlantic Ocean as simulated with a realistic general circulation model that uses the historical data set [*Levitus*, 1982] as initial data. A detailed description of the model is given in a companion paper by *Philander and Pacanowski* [this issue]. This model differs from the one recently used by *Sarmiento* [1986] to simulate the seasonal cycle of the entire Atlantic Ocean in two respects. Whereas Sarmiento's model resolves the oceanic eddies in neither low nor high latitudes, this model has sufficiently high resolution in the tropics to resolve the eddies there. (The focus in this study is entirely on the region 15°N to 15°S.) The second difference between the two models concerns the surface boundary condition. *Sarmiento* [1986] specifies sea surface temperature and uses the model to determine the heat flux that is consistent with the sea surface temperature. This approach is problematic in a model that resolves the equatorial eddies because the eddies have a large signature in the sea surface temperature field. We therefore specify the meteorological variables needed to calculate the surface heat flux so that the model predicts the sea surface temperature. The surface heat fluxes in the model and in Sarmiento's model are compared in section 3.

2. The Mass Budget

Figure 1 is a schematic diagram of the circulation in the tropical Atlantic Ocean. The principal nonzonal current is the northwestward flowing Brazilian Coastal Current. It absorbs water from the westward South Equatorial Current, which occupies the region to the south of 3°N. The Brazilian Coastal Current in turn feeds the eastward Equatorial Undercurrent and the North Equatorial Countercurrent between 3°N and 10°N approximately. The countercurrent loses some of its water to northward Ekman drift, but most of it is lost to downwelling into the thermocline. There the motion is equatorward, toward the Equatorial Undercurrent, which in turn loses fluid because of equatorial upwelling to the South Equatorial Current. To quantify this circulation the model ocean is divided into the boxes shown in Figure 2. A triad of numbers in this figure denotes the annual mean fluxes across a vertical surface in the upper 50 m, between 50 m and 317 m, and below 317 m, respectively. (A minus sign means that the flux is opposite to the direction of the arrow.) Figure 2 shows that the northward mass flux of the Brazilian Coastal Current (the flux in the upper 317 m of the ocean to the west of 30°W) increases from 18.8 to 25.4 Sv between 5°S and 2.5°S. It then decreases to 15.5 Sv across 2.5°N as mass is lost to the Equatorial Undercurrent, and it decreases

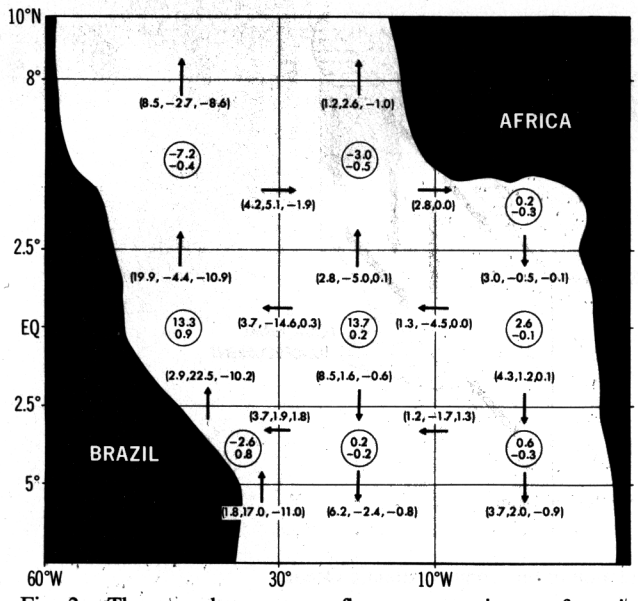

Fig. 2. The annual mean mass flux across various surfaces in the model. A triad of numbers indicate the flux in the upper 50 m, between 50 m and 317 m, and below 317 m, in sverdrups. A minus sign indicates that the flux is opposite to the direction of the arrow. The numbers in the circles are the vertical mass fluxes (positive is upward) in sverdrups across horizontal surfaces at 50 m (top number) and 317 m (bottom number).

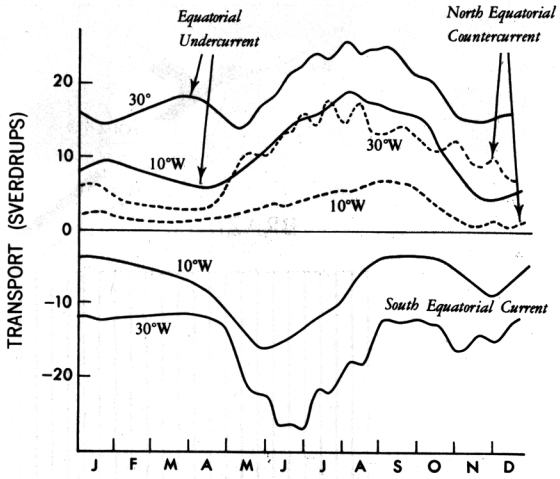

Fig. 3. Transport (10^6 m^3 s^{-1}) of the currents across 30°W and 10°W, above 317 m and north of 10°S, as defined by the zero zonal velocity contours. Positive values indicate eastward flow. The upper solid lines are for the Equatorial Undercurrent; the lower solid lines for the South Equatorial Current. The dashed lines are for the North Equatorial Countercurrent.

further to 5.8 Sv across 8°N as mass is lost to the countercurrent. The eastward transport between 2.5°N and 8°N decreases in a downstream direction not because of a loss to northward Ekman drift (the Ekman drift across 2.5°N exceeds that across 8°N) but because of downwelling and then equatorward flow at the depth of the thermocline into the Equatorial Undercurrent. (In Figure 2 the top and bottom numbers in circles give the vertical transports in sverdrups across 50 m and 317 m, respectively. A minus sign indicates downwelling.) Some of the countercurrent water (2.8 Sv is the annual mean) penetrates into the Gulf of Guinea, where it flows across the equator into the southern hemisphere. The Equatorial Undercurrent, although it gains mass from the north as it flows eastward, reduces its transport from 14.6 Sv across 30°W to 4.5 Sv across 10°W because of equatorial upwelling. (These numbers refer to the transport between 50 m and 317 m, 2.5°N and 2.5°S.) The upwelled water augments the westward flow of the South Equatorial Current in the surface layers of the equatorial zone and sustains the divergent Ekman drift, especially into the southern hemisphere, where it is swept westward toward the Brazilian Coastal Current.

The estimates for the transports of the various currents in Figure 2 are approximate because the grid does not coincide with the boundaries of the currents. The line along 2.5°N, for example, cuts through deep, intense westward flow that is part of the South Equatorial Current. Figure 3 depicts the transports of the currents across 30°W and 10°W, to the north of 10°S and above 317 m, as defined by the zero zonal velocity component contour. The downstream decrease in the transport of the eastward currents and the downstream increase in the transport of the westward South Equatorial Current are evident.

Equatorial upwelling and strong downwelling between 2.5°N and 8°N clearly play an important role in the oceanic circulation. What is surprising in Figure 2 is the intensity of the upwelling in the western equatorial Atlantic where sea surface temperatures are at a maximum. Upwelling in this region has relatively little effect on sea surface temperatures because it has a maximum at a depth near 50 m and attenuates rapidly with increasing depth (Figure 4). The upwelling has considerable spatial and temporal variability, on scales of 1000 km and 1 month approximately, associated with waves caused by instabilities of the surface currents [*Philander et al.*, this issue]. Spatial averages minimize this variability and reveal that the seasonal changes in equatorial upwelling are very different in the east and west. The eastern equatorial Atlantic has a distinct semiannual cycle of upwelling and downwelling which is only partially attributable to semiannual changes in the wind [*Philander and Pacanowski*, this issue]. This equatorial upwelling and downwelling in the Gulf of Guinea is highly correlated with variations in the westward flux of mass in the upper 50 m across 10°W (Figure 5). In other words, equatorial upwelling in the Gulf of Guinea is primarily associated with the divergence of the westward surface flow, not with the divergence of the meridional Ekman drift. In the western equatorial Atlantic, upwelling is

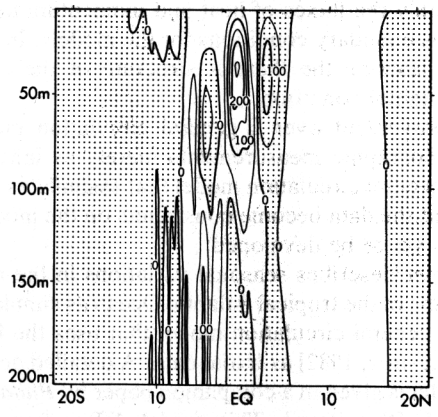

Fig. 4. The annual mean vertical velocity component (positive is upward), in centimeters per day, along 30°W.

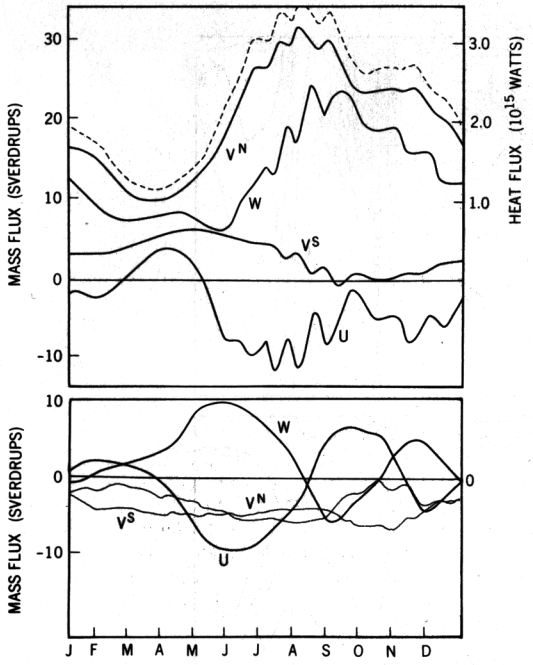

Fig. 5. Time dependence of the mass fluxes in sverdrups (= 10^6 m^3 s^{-1}) across the faces of boxes in the (top) western and (bottom) eastern equatorial zones. The western box extends from the Brazilian coast to 30°W, from 2.5°N to 2.5°S, and from the surface to 50 m. The eastern box has the same vertical and latitudinal extent but extends from 10°W to the African coast. The zonal flux U is eastward if positive; the meridional fluxes V^N and V^S across the northern and southern faces, respectively, are northward if positive, and the vertical flux W is upward if positive. The dotted line in the top figure is the heat flux across the northern face.

highly correlated with the seasonal changes in the local winds and is most intense between July and October when the local westward winds are most intense. During this period, northward flow out of the equatorial zone across 2.5°N is at a maximum, but northward flow across 8°N is at a minimum (Figure 6). This convergence of mass implies intense downwelling between 2.5°N and 8°N in the west during the months when the Brazilian Coastal Current veers offshore near 5°N. The downwelled water flows back southward (Figure 6) into the Equatorial Undercurrent which in turn loses it because of equatorial upwelling, as was described earlier. A simplified version of this complex circulation emerges if the equation for the conservation of mass is integrated zonally so that a stream function for the meridional circulation can be introduced. Figure 7 shows this stream function in mid-August and mid-February. Below a depth of 1500 m there is southward flow, between 10 and 20 Sv, across all latitudes. The return northward flow in the upper 1500 m has a complex vertical and temporal structure. In the southern hemisphere the northward flow is between 50 m and 1500 m and amounts to 25 Sv approximately because the surface layers have a southward Ekman transport of 10 Sv approximately. Near the equator, upwelling brings some of the deep northward flow into the surface layers to maintain the southward Ekman drift. During those months (December to May) when the Brazilian Coastal Current flows continuously into the Gulf of Mexico, equatorial upwelling brings additional deep northward flowing water into the surface layers, where it continues northward. During the remaining months, when the Brazilian Coastal Current veers offshore near 5°N, equatorial upwelling is much more intense, but it is merely part of a shallow meridional cell with intense downwelling near 3°N. The equatorial upwelling of deep water is actually reduced during these months, and instead there is upwelling of deep water near 10°N. From Figure 2 it is clear that both the shallow and deep meridional flow are predominantly near the Brazilian coast.

3. Heat Flux Across the Ocean Surface

The heat flux across the ocean surface in the model varies primarily because of changes in the latent heat lost by the ocean. (The sensible heat lost is negligible, and the solar radiation is assumed to be a constant, as is described in section 2 of *Philander and Pacanowski* [this issue].) The loss of latent heat depends on the wind speed and on the temperature difference between the sea surface and the adjacent air. The air temperature is specified from climatological data. The model predicts the sea surface temperature.

Far from the equator the ocean gains heat during summer and loses heat during winter. Figure 8 shows that this is true to within 10° latitude of the equator. Between 3°N and 6°S approximately, the ocean gains heat throughout the year, especially in July and August in the central part of the basin where equatorial upwelling is intense and sea surface temperatures are low. In the region of the North Equatorial Countercurrent the ocean loses heat in July and August when that current is most intense. The shear between the eastward countercurrent and the adjacent westward South Equatorial Current results in instabilities which appear as westward traveling waves in the sea surface temperature

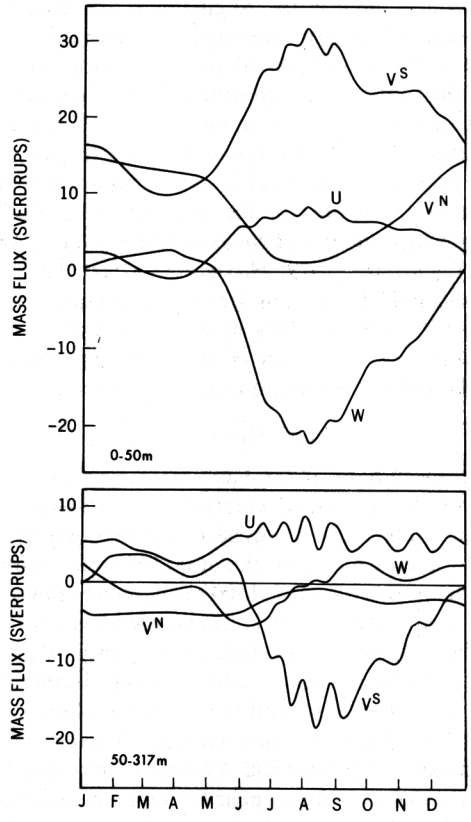

Fig. 6. As in Figure 5 but for boxes bounded by 2.5°N and 8°N, the Brazilian coast, and 30°W. The top panel extends from the surface to 50 m; the bottom panel extends from 50 m to 317 m.

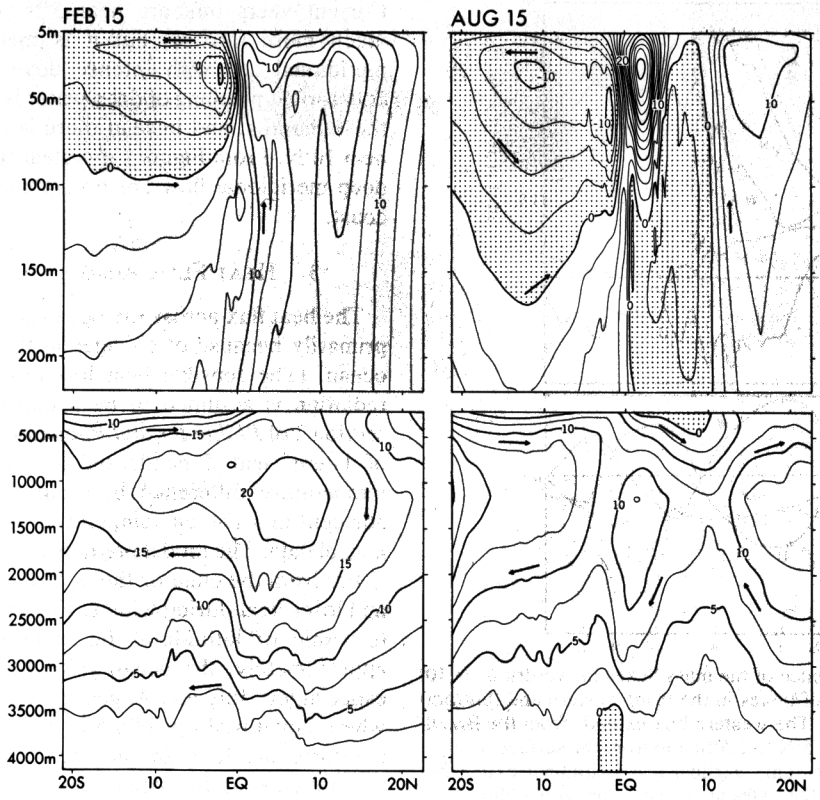

Fig. 7. Stream function for the zonally integrated mass flux on February 15 and August 15. The difference between two contours is the transport in units of 2.5 Sv.

patterns and which affect the heat flux across the ocean surface as is evident in the August map of Figure 8.

The oceanic heat gain averaged over a year is essentially confined to the neighborhood of the equator, as in *Sarmiento*'s [1986] model that specifies sea surface temperature rather than heat flux as an upper boundary condition. The two models are in good agreement in the tropics, although the heat gained in this model is somewhat lower than it is in Sarmiento's. Estimates of the oceanic heat gain that are based on measurements [*Esbensen and Kushnir*, 1981; *Bunker and Goldsmith*, 1979; *Hastenrath*, 1980, 1982] indicate that the latitudinal extent of the region that gains heat is too small in both models. This model should improve with a more realistic specification of the incoming radiation and relative humidity (which are taken to be constants).

4. The Heat Budget

The northern hemisphere has a northward heat transport because the warm surface waters move northward while the cold deep water moves equatorward (section 2). To the south of the equator, both the surface layers (above 50 m) and the deep ocean (below 1500 m) move southward, while the fluid at intermediate depth moves northward. The direction of the heat flux is therefore unclear until two important zonal variations are taken into account: isotherms slope downwards to the west, and the northward flow is concentrated in a western boundary current. Because of this the heat transport in the tropical Atlantic is northward in both hemispheres and increases near the equator, where there is always a flux of heat into the ocean. Figure 9 quantifies this latitudinal variation in the northward heat flux. Figure 10 shows the heat budget for the different boxes into which the model ocean has been divided. Figure 10 does not include heat diffusion, which is most important near the temperature front along 3°N, where it causes a southward flux of the order of 0.2 PW = 2×10^{14} W. (It is not possible to calculate a useful average temperature for all the surfaces from the number in Figures 2 and 10 because the flow across some of the surfaces is not uniformly in one direction. For example, across the surface from 2.5°N to 2.5°S and from 0 m to 50 m, there is westward flow near the ocean surface and eastward flow below that. The average temperature of that surface can therefore not be obtained from the integrated mass and heat fluxes across that surface.) Figure 10 confirms the significant zonal variations in the heat flux: the meridional flux is predominantly in the western side of the basin. From Figure 10 it is also evident that the heat flux in the deep ocean is so small that variations in the temperature or velocity of the deep ocean are unlikely to have a significant effect on the heat transport. *Roemmich* [1983] has come to a similar conclusion.

In Figures 6 and 7 we noted that the variability of the mass flux is predominantly on two time scales: seasonal and monthly. The same is true of the heat flux. In fact, the variations in the heat flux across a given surface are almost identical to the variations in the mass flux. (See, for example, the dotted line in Figure 5.) The reason is the following. The meridional heat flux is proportional to

$$VT = \overline{V}\,\overline{T} + V'\overline{T} + \overline{V}T' + V'T'$$

The temperature variations T' are far smaller than the time-averaged temperature $\overline{T}$, but the meridional velocity fluctuations V' are greater than the time-averaged meridional flow $\overline{V}$. Hence $V'\overline{T}$ is the dominant time-dependent term in

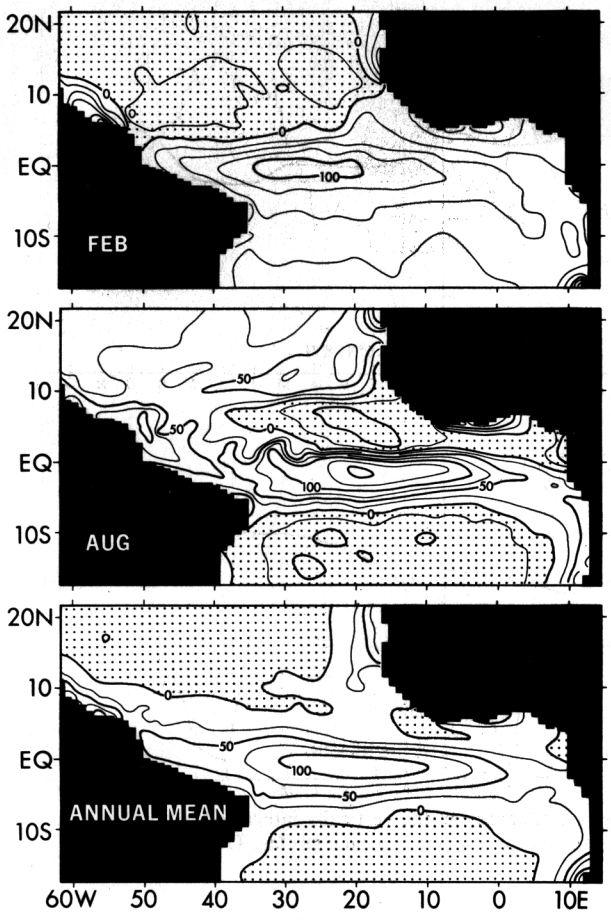

Fig. 8. The heat flux across the ocean surface (in watts per square meter; in negative regions the ocean loses heat) on February 15 and August 15. The bottom figure shows the annual mean.

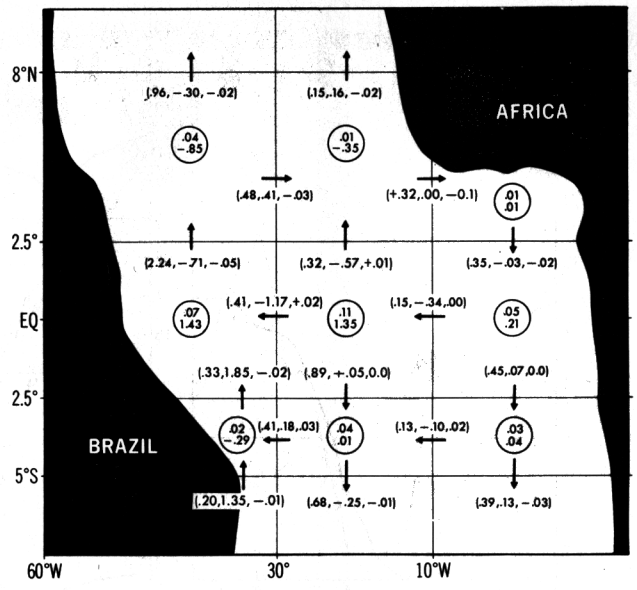

Fig. 10. As in Figure 2 but for the annual mean heat flux in units of 10^{15} W. In the circles the upper number is the heat flux across the ocean surface, and the lower number is the heat transport across the horizontal surface at 50 m. Diffusive fluxes are not included in these numbers.

the above equation, so that the variations in the heat flux are similar to V', the variations in the mass flux. In time averages (over a year) of the heat flux the term $V'T'$ becomes very important. Of special interest is the heat flux associated with the oceanic eddies which have a time scale of a month approximately. These eddies appear as westward traveling waves on the temperature front near 3°N in the western side of the basin. Motion in the cold crests of the waves, which point northward, is northward and downward, while motion in the warm troughs is southward and upward [*Philander et al.*, this issue, Figure 5]. The meridional motion implies a southward heat flux by the eddies; the vertical motion implies that they effect an upward heat flux. The waves are extremely energetic for a short period, 2 months approximately, so that their contribution to the annual mean heat flux is very small. Across 2.5°N, it is estimated to be 0.1 PW at most, which is small in comparison with the northward flux of 1 PW across that latitude shown in Figure 9 [*Philander et al.*, this issue].

The heat transport across 5°S and across 15°N has little seasonal variation (Figure 11). Across 8°N, however, the northward flux varies from 1.75 PW in January, when the Brazilian Coastal Current flows continuously into the Gulf of Mexico, to −0.2 PW in August, when this current veers offshore near 5°N. The highly variable flux across 8°N and the relatively steady fluxes across 5°S and 8°N imply that the two latitudinal bands 5°S to 8°N and 8°N to 15°N act as capacitors that are out of phase. During those months when the heat transport across 8°N is small, the zone 5°S to 8°N

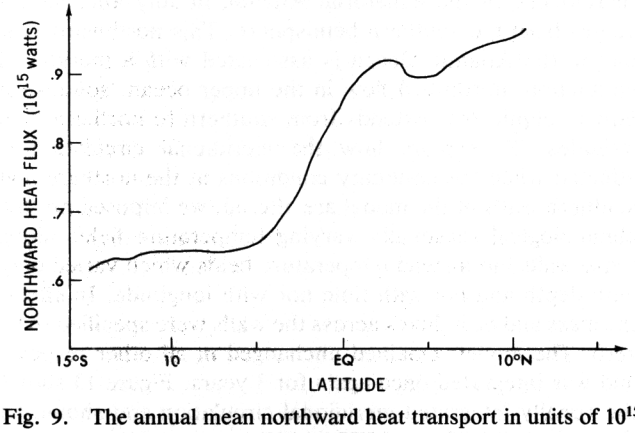

Fig. 9. The annual mean northward heat transport in units of 10^{15} W (= 1 PW).

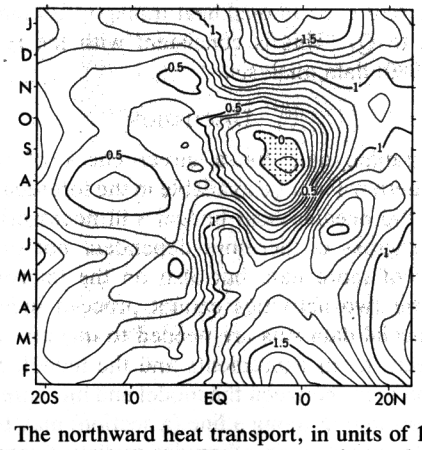

Fig. 11. The northward heat transport, in units of 10^{15} W, as a function of time and latitude. The transport is southward in the shaded area.

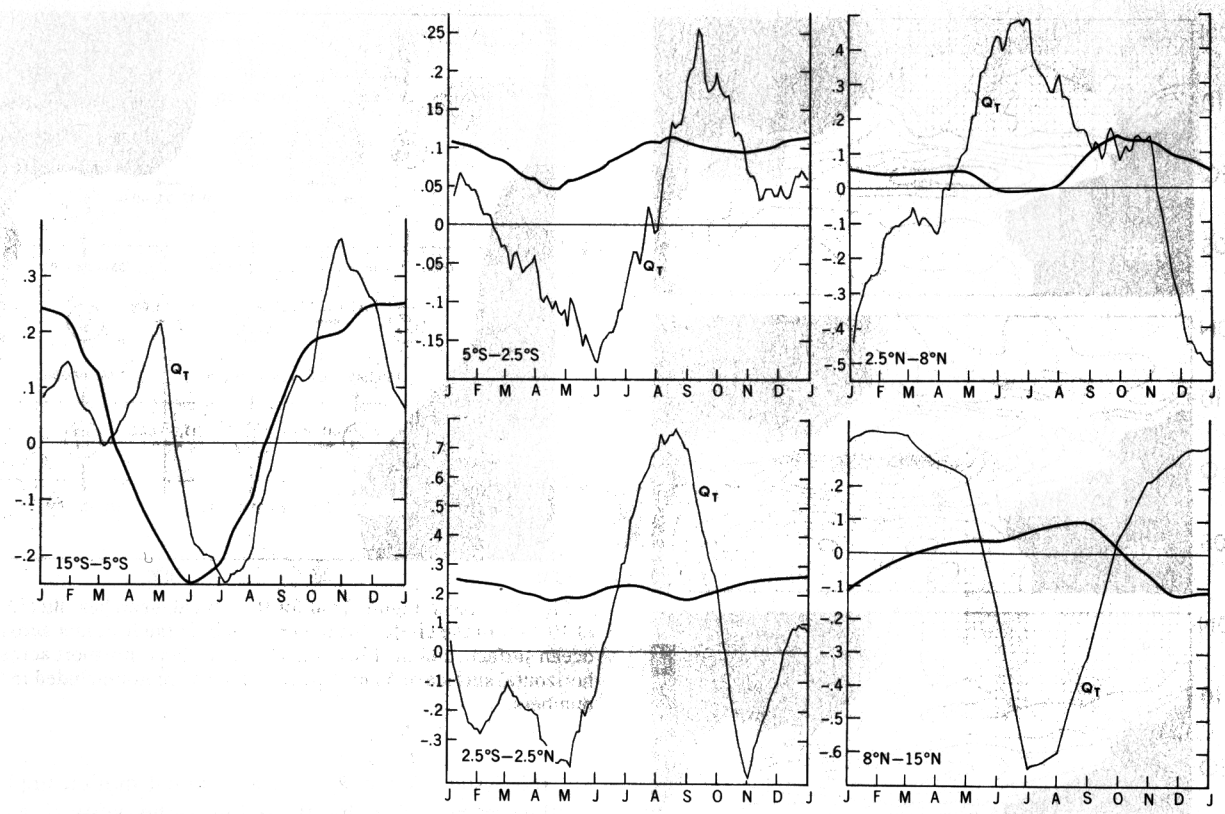

Fig. 12. The heat flux across the ocean surface and Q_T, the rate of change of the vertically integrated temperature in zonal boxes bounded by the American and African continents and by the indicated latitude circles. The units are 10^{15} W.

stores heat obtained from the southern hemisphere, so that the thermocline in that region deepens. During this period the heat stored in the band 8°N to 15°N is released, so that the thermocline shoals, in order to maintain the heat flux across 15°N. An elevation of the thermocline in the band 5°S to 8°N from October until May permits a large flux of heat across 8°N and replenishment of the heat content of the band 8°N to 15°N. Figure 12 shows the changes in the heat content Q of different zonal bands and also shows the heat flux F across the ocean surface in each band. To the south of 5°S the rate of change of Q is very similar in phase and amplitude to F. In other words, the rate of change of heat storage is determined principally by the heat flux across the ocean surface. Between 5°S and 15°N this is not so because the divergence of the meridional heat transport is comparable in magnitude to Q_T. This is consistent with the results from *Merle*'s [1980] data analysis.

5. Discussion

Oceanographic data for a direct check of the results presented here will not be available in the foreseeable future; studies of the oceanic heat budget will necessarily involve models. Progress is therefore dependent not only on the acquisition of more data but also on the improvement of models. The two activities cannot proceed independently because special data sets are needed to quantify discrepancies between the measurements and the model. For example, disagreement between the model and measurements at a point (a mooring) or along a line (a section) may be due to a slight displacement of an otherwise realistic spatial pattern. The data should be sufficient to describe the pattern. Once the flaws of the model are diagnosed, remedial steps can be taken, improvement of the mixing parameterization, for example. Because of the known flaws of the model, the absence of deep Equatorial Countercurrents near 5°N and 5°S, for example [*Hisard et al.*, 1976; *Molinari*, 1982], the quantitative results presented here will change when the model improves. The qualitative results that are unlikely to change include the role of upwelling and downwelling in closing the oceanic circulation, the large seasonal changes in the heat transport across 8°N, and the opposite phases of changes in heat storage in the regions to the north and south of 8°N.

The results described here indicate that conditions outside the tropics can affect oceanic conditions in the tropical oceans. Some of the heat for the deepening of the thermocline in the equatorial Atlantic in July and August comes from the southern hemisphere. This northward heat flux in the Atlantic Ocean is associated with a meridional circulation, northward flow in the upper ocean, southward flow at depth, that extends from southern to northern high latitudes. To explore how the meridional circulation is affected when the boundary conditions at the northern and southern walls of the model are altered, we imposed not the climatological seasonally varying temperature fields along those walls but instead temperature fields which varied only with depth and not with time nor with longitude. In effect, the mass and heat fluxes across the walls were specified to be zero. The model remained unchanged in all other respects and was integrated once again for 3 years. Figure 13 shows the zonally integrated meridional circulation and should be contrasted with Figure 7. Motion in the upper 150 m near the

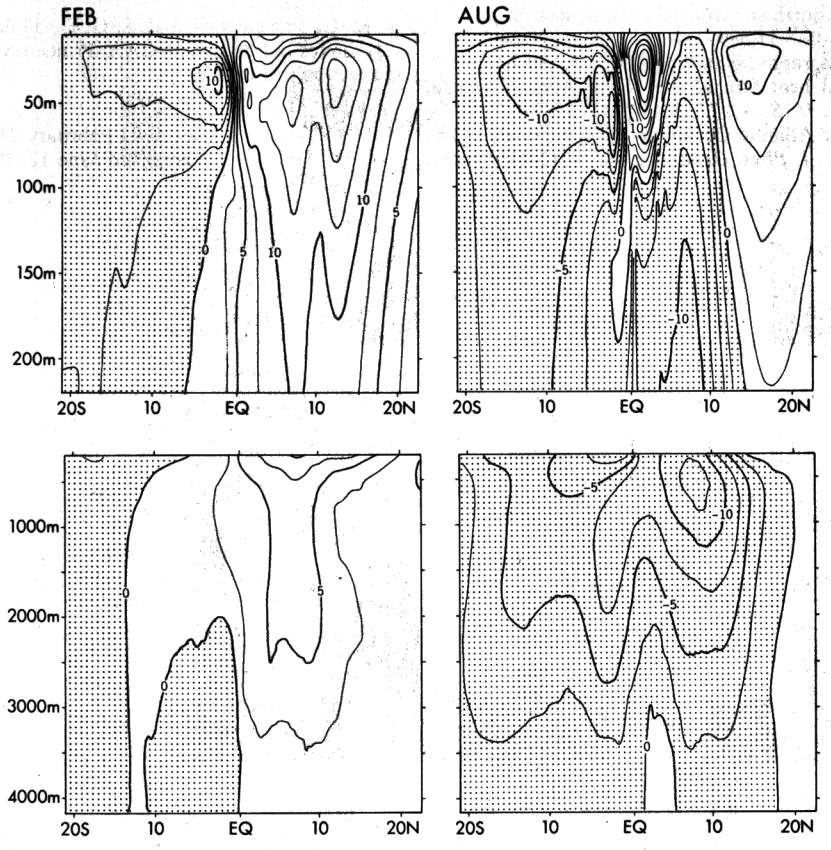

Fig. 13. As for Figure 7 except for a change in the boundary conditions at the northern and southern walls. See text.

equator is unaffected, but the deep southward transport from high northern to high southern latitudes disappears. This causes a large change in the heat flux which changes from northward in both hemispheres (Figure 9) to poleward in each hemisphere.

The Atlantic Ocean is believed to gain heat from the Indian Ocean by means of Agulhas Current eddies that drift around the southern tip of Africa [*Gordon*, 1986]. The model results suggest that variations in the heat flux across 35°S could affect the heat transport further north on the relatively short time scale of a few seasons. Although results for the third year of the integration were not significantly different from those during the second year, it is probable that integrations over much longer periods, several decades, will show significant gradual changes. Further studies are needed to determine whether conditions in high latitudes can affect the upper tropical oceans and to determine the time scales on which this happens.

Acknowledgments. K. Bryan made valuable comments on an earlier version of this paper. P. Tunison and J. Pege provided expert technical assistance with the preparation of the paper.

REFERENCES

Bennett, A. F., Poleward heat fluxes in southern hemisphere oceans, *J. Phys. Oceanogr.*, *8*, 785–798, 1978.

Bryan, K., Measurements of meridional heat transport by ocean currents, *J. Geophys. Res.*, *67*, 3403–3414, 1962.

Bryan, K., Poleward heat transport by the ocean: Observations and models, *Annu. Rev. Earth Planet. Sci.*, *10*, 15–38, 1982.

Bunker, A., and R. A. Goldsmith, Archived Time-Series of the Atlantic Ocean Meteorological Variables and Surface Fluxes, Rep. *WHOI-79-3*, 28 pp., Woods Hole Oceanogr. Inst., Woods Hole, Mass., 1979.

Esbensen, S. K., and Y. Kushnir, The heat budget of the global ocean, An atlas based on estimates from marine surface observations, 208 pp., Oreg. State Univ., Corvallis, 1981.

Gordon, A. L., Interocean exchange of thermocline water, *J. Geophys. Res.*, *91*, 5037–5046, 1986.

Hastenrath, S., Heat budget of tropical oceans and atmospheres, *J. Phys. Oceanogr.*, *10*, 157–170, 1980.

Hastenrath, S., On meridional heat transport in the world ocean, *J. Phys. Oceanogr.*, *12*, 922–927, 1982.

Hisard, P., J. Citeau, and A. Morlière, Le système des contre courants équatoriaux de subsurface, *Cah. ORSTOM, ser Oceanogr.*, *14* (3), 209–220, 1976.

Levitus, S., Climatological atlas of the world ocean, *NOAA Prof. Pap. 13*, 173 pp., U.S. Government Printing Office, Washington, D. C., 1982.

Merle, J., Seasonal heat budget in the equatorial Atlantic Ocean, *J. Phys. Oceanogr.*, 464–469, 1980.

Molinari, R. L., Observations of eastward currents in the tropical South Atlantic Ocean: 1978–1980, *J. Geophys. Res.*, *87*, 9707–9714, 1982.

Philander, S. G. H., and R. C. Pacanowski, Simulation of the seasonal cycle in the tropical Atlantic Ocean, *Geophys. Res. Lett.*, *11*, 802–804, 1984.

Philander, S. G. H., and R. C. Pacanowski, A model of the seasonal cycle of the tropical Atlantic Ocean, *J. Geophys. Res.*, this issue.

Philander, S. G. H., and A. D. Seigel, Simulation of El Niño of 1982–1983, in *Coupled Ocean-Atmosphere Models*, edited by J. Nihoul, pp. 517–541, Elsevier, New York, 1985.

Philander, S. G. H., W. J. Hurlin, and R. C. Pacanowski, Properties of long equatorial waves in models of the seasonal cycle in the tropical Atlantic and Pacific oceans, *J. Geophys. Res.*, this issue.

Roemmich, D., The balance of geostrophic and Ekman transports in the tropical Atlantic Ocean, *J. Phys. Oceanogr.*, *13*, 1534–1539, 1983.

Sarmiento, J. L., On the north and tropical Atlantic heat balance, *J. Geophys. Res.*, *91*, 11,677–11,689, 1986.
Sverdrup, H. U., Oceanography, *Handb. Physik*, *48*, 630–638, 1957.
Wunsch, C., Meridional heat flux of the North Atlantic Ocean. *Proc. Natl. Acad. Sci. U. S. A.*, *77*, 5043–5047, 1980.
Wunsch, C., An eclectic Atlantic Ocean circulation model, I, The meridional flux of heat, *J. Phys. Oceanogr.*, *14*, 1712–1733, 1984.

R. C. Pacanowski and S. G. H. Philander, Geophysical Fluid Dynamics Laboratory, NOAA, Princeton University, P.O. Box 308, Princeton, NJ 08542.

(Received February 24, 1986;
accepted June 12, 1986.)